T·H·E OHIO STATE UNIVERSITY

SMI ADAPTIVE ANTENNA ARRAYS FOR WEAK INTERFERING SIGNALS

I.J. Gupta

The Ohio State University

ElectroScience Laboratory

Department of Electrical Engineering
Columbus, Ohio   43212

NOTICES

When Government drawings, specifications, or other data are used for any purpose other than in connection with a definitely related Government procurement operation, the United States Government thereby incurs no responsibility nor any obligation whatsoever, and the fact that the Government may have formulated, furnished, or in any way supplied the said drawings, specifications, or other data, is not to be regarded by implication or otherwise as in any manner licensing the holder or any other person or corporation, or conveying any rights or permission to manufacture, use, or sell any patented invention that may in any way be related thereto.

50272-101

REPORT DOCUMENTATION PAGE	1. REPORT NO.	2.	3. Recipient's Accession No.

4. Title and Subtitle	5. Report Date
SMI ADAPTIVE ANTENNA ARRAYS FOR WEAK INTERFERING SIGNALS	September 1987
	6.

7. Author(s)	8. Performing Organization Rept. No.
I.J. Gupta	716111-5

9. Performing Organization Name and Address	10. Project/Task/Work Unit No.
The Ohio State University ElectroScience Laboratory 1320 Kinnear Road Columbus, Ohio 43212	
	11. Contract(C) or Grant(G) No
	(C) NAG 3-536
	(G)

12. Sponsoring Organization Name and Address	13. Type of Report & Period Covered
National Aeronautics and Space Administration Lewis Research Center 21000 Brookpark Road Cleveland, Ohio 44135	Technical
	14.

15. Supplementary Notes

16. Abstract (Limit: 200 words)

The performance of adaptive antenna arrays is studied when sample matrix inversion (SMI) algorithm is used to control array weights. It is shown that conventional SMI adaptive antennas, like other adaptive antennas, are unable to suppress weak interfering signals (below thermal noise) encountered in broadcasting satellite communication system. To overcome this problem, the SMI algorithm is modified. In the modified algorithm, the covariance matrix is modified such that the effect of thermal noise on the weights of adaptive array is reduced. Thus, the weights are dictated by relatively weak coherent signals. It is shown that the modified algorithm provides the desired interference protection. The use of defocused feeds as auxiliary elements of an SMI adaptive array is also discussed.

17. Document Analysis   a. Descriptors

b. Identifiers/Open-Ended Terms

c. COSATI Field/Group

18. Availability Statement	19. Security Class (This Report)	21. No. of Pages
Approved for public release; distribution is unlimited.	Unclassified	57
	20. Security Class (This Page)	22. Price
	Unclassified	

(See ANSI-Z39.18)   See Instructions on Reverse

OPTIONAL FORM 272 (4-77)
(Formerly NTIS-35)
Department of Commerce

TABLE OF CONTENTS

PRECEDING PAGE BLANK NOT FILMED

iv

LIST OF FIGURES

I. INTRODUCTION

A major problem in satellite communications is the interference caused by transmission from adjacent satellites whose signals inadvertently enter the receiving system and interfere with the communication link. The same problem arises in the earth to satellite part of the link where transmission from nearby ground stations enter the satellite receiver through its antenna sidelobes. The problem has recently become more serious because of the crowding of the geostationary orbit. Indeed this interference prevents the inclusion of additional satellites which could have been allowed if methods to suppress such interference were available. The interference can be suppressed at the originating station, either space or earth, by lowering the sidelobes of the transmitting antenna. Alternatively, the interfering signals may be suppressed at the receiving site. Under the present grant, we are examining the latter approach. The undesired signal sources (interfering signals) are assumed to be located at arbitrary angular separations from the desired signal source. The spectral characteristics and modulations of the desired and undesired signals are similar. The signal-to-noise ratio (SNR) of the desired signal is expected to be 15 dB. The undesired signals are 10-30 dB below the desired signal level (unintentional interference). Thus, the undesired signals are significantly weaker than the desired signal and in fact may even be below the noise level by several dB. Although weak, these signals because of their coherent nature and their similarity to the desired signal, do cause objectionable interference.

1

Adaptive antenna arrays [1-5] have been used to provide protection to radar and communication systems from undesired signals. Undesired signals may consist of deliberately generated electronics counter measure signals, unintentional RF interference, clutter scatter returns and natural noise sources. An adaptive array automatically steers nulls onto sources of undesired signals while attempting to retain the desired main beam characteristics in the desired signal direction and thus maximizes the output signal-to-interference-plus-noise ratio (SINR). The output SINR is optimized in real-time, making adaptive arrays useful in a changing interference environment. In the present application, the exact location of interfering sources are a priori unknown and may change with time. Therefore, an adaptive array is suitable to provide interference protection. Also since the spectral characteristics and modulation of the desired signal and undesired signal are similar, while the desired signal source location is known, steered beam type adaptive arrays [2] should be used to provide interference protection. The performance of steered beam adaptive arrays in the presence of weak interfering signals was studied in our earlier work [6,7]. It was shown that the conventional adaptive arrays may not provide the desired interference suppression[*]. The reason for this is that the interfering signals are relatively weak. In the case of weak interfering signals, the thermal noise (sky noise and/or internal thermal noise) is the main

---

* The performance of steered beam adaptive arrays was studied. However, the results are also true for LMS adaptive arrays of Widrow et al. [1].

2

source of degradation in the output SINR and thus it (thermal noise) dictates the array weights. The array adjusts its weights to minimize the thermal noise which in turn maximizes the output SINR; however, the interfering signals remain unsuppressed. To overcome this difficulty, a modification to the feedback loops controlling the array weights was proposed. It was shown that the modified feedback loops provide the required interference suppression.

The steered beam type adaptive arrays can also be implemented using sample matrix inversion (SMI) algorithm [8,9]. The conventional SMI adaptive antenna arrays, as shown in this report, face the same problem; i.e., one may not obtain the required suppression of weak interfering signals. To overcome this difficulty, a modification to the SMI algorithm is proposed. It is shown that the modified SMI algorithm provides the required interference suppression.

In the modified SMI algorithm, the sample covariance matrix [8,9] is modified to reduce the effect of thermal noise on the weights of the adaptive array. This is accomplished by subtracting a fraction of the smallest eigenvalue of the original covariance matrix from its diagonal terms. In situations where the number of degrees of freedom of adaptive arrays is larger than the number of interfering signals, the smallest eigenvalue of the sample covariance matrix is equal to the noise power in the individual antenna elements. Thus, subtracting a fraction of the smallest eigenvalue from the diagonal terms of the covariance matrix is equivalent to reducing the thermal noise in individual antenna elements which in turn increases the input interference-to-noise ratio (INR). The adaptive array, therefore, will respond to the interfering signals

3

and will suppress them. The larger the input INR, the larger the interference suppression [3]. Thus, by adjusting the fraction of the smallest eigenvalue which is subtracted from the diagonal terms, one can obtain the required interference suppression.

The remaining part of this report is organized as follows. The performance of a conventional SMI adaptive array is discussed in Section II. Sections III and IV deal with modified SMI algorithm. In Section V, it is shown that when the main antenna is a reflector antenna, one can use offset feeds as auxiliary elements of a modified SMI adaptive array.

II. A CONVENTIONAL SMI ADAPTIVE ARRAY

In this section, the interference protection provided by a conventional steered beam type adaptive antenna array (SMI algorithm is used) to a communication system is studied. It is shown that such an adaptive array is unable to suppress weak interfering signals. Some modifications in the adaptive array are, therefore, needed. Consider the simple schematic shown in Figure 1. In Figure 1, the antenna array consists of a main antenna and M auxiliary antennas. The main antenna is highly directive and is steered in the desired signal direction. The auxiliary antennas are relatively low gain antennas and may have approximately uniform radiation in the given sector. The signals received by each of these antennas are multiplied by a complex weight w_k and are then added to form the output signal. The complex weights, w_k, are computed using the well known SMI algorithm [8,9]. The weights of the adaptive array are given by

4

$$W = \mu\hat{\Phi}^{-1}S \tag{1}$$

where W is the adaptive weight vector,

$\hat{\Phi}$ is the sample covariance matrix,

S is the steering vector [2] and

μ is a constant.

The sample covariance matrix, $\hat{\Phi}$, is computed via the simple "block" average over N snapshots

$$\hat{\Phi} = \frac{1}{N}\sum_{n=1}^{N} X(n)X^{\dagger}(n) \tag{2}$$

where X(n) is the element signal data vector received at the nth time sampling and superscript $\dagger$ denotes transpose of complex conjugate. In this study, N is assumed to be large so that $\hat{\Phi}$ does not change from one update to another update (assuming the signal scenario remains unchanged). The steering vector S is chosen such that the quiescent pattern of the array has its main beam in the desired signal direction and leads to the maximum SNR in the absence of interfering signals. One should know the desired signal direction and its relative amplitude at the various antenna elements to choose a proper steering vector. In the case of ground station or satellite receiver antennas, the location of the desired signal source is known and one can find the desired signal amplitude at the various antenna elements by knowing the gain of the various antennas in the desired signal direction.

5

In practice, the signals incident on the various antenna elements consist of a desired signal, interfering signals and uncorrelated noise (sky noise and/or internal thermal noise). Assuming that the various signals incident on the array are uncorrelated with each other and the noise, and the noise voltages in various antennas are uncorrelated with each other and are zero mean Gaussian with variance σ^2, one can compute the covariance matrix $\hat{\Phi}$, and the steady state weights can be found. Knowing the steady state weights, the performance of the adaptive array can be evaluated. In this study, $\hat{\Phi}$ is assumed to be known exactly.

Figure 2 shows the output INR of a SMI adaptive array consisting of four auxiliary antennas. The auxiliaries are assumed to be isotropic antennas with interelement spacing of half a wavelength. The main antenna is a reflector antenna and is steered along the desired signal's direction (broadside to the array). The SNR of the desired signal in the main antenna is assumed to be 14.6 dB while it is -10 dB in the auxiliary antennas. The interfering signal scenario consists of a single CW interfering signal incident from 30° off broadside to the array. The main antenna has a -16.6 dB sidelobe in this direction; i.e., if the desired signal is incident from this direction, the SNR in the main antenna will be -2 dB instead of 14.6 dB. The output INR is plotted versus the input INR in the main antenna. The input INR in each auxiliary antenna is 8 dB below its value in the main antenna[*]. Note that for weak interfering signals (input INR < -5 dB), the output INR is

---

* The thermal noise is assumed to be of the same level in all antennas.

6

approximately equal to the INR at the main antenna input. Thus, the interfering signal is not suppressed by the array. The reason for no interference suppression is discussed below.

For weak interfering signals, the thermal noise is the main source of degradation in the output SINR. Therefore, the array weights are adjusted to maximize the SNR. The steering vector, S, leads to the maximum SNR. Thus, in the presence of weak interfering signals, the array weights remain unchanged and no interference suppression is obtained. Therefore, some modifications in the adaptive array are needed to suppress weak interfering signals.

When the directions of sources radiating the interfering signals are approximately known, one can replace the low gain auxiliary antennas with high gain antennas and can point their beams in those directions. Thus, the interference signal level in the auxiliaries will increase and their weights will be controlled by the interfering signals. The weights will be adjusted to suppress the interfering signals. The larger the gain of the auxiliary antennas, the higher the interference suppression (approximately equal to output INR/input INR (Main)). This can be seen in the plots of Figure 3. In this figure, the output INR of the 4-auxiliary element adaptive array is plotted when the auxiliary antennas are directive antennas with a gain G_a in the interference direction. Thus, input INR in each auxiliary antenna is G_a dB higher than its value in Figure 2. All other parameters are the same as in Figure 2. Note that the output INR decreases with an increase in the gain of auxiliary antennas. However, for weak interfering signals, INR (main) $\leq$ -5 dB, one needs very high gain auxiliary antennas to suppress

7

the interfering signals by 20-30 dB, which may not be practical. To achieve such gain, the auxiliary antennas may have to be larger than the main antenna. Other methods of interference suppression, therefore, should be explored. A modification to the SMI algorithm used to compute the array weights is proposed next. It is shown that the modified SMI algorithm can provide the required interference suppression.

III. MODIFIED SMI ALGORITHM

Let λ_i, $i=1,2,\ldots M+1$ be the eigenvalues of the covariance matrix, $\hat{\Phi}$, with e_i, $i=1,2,\ldots M+1$ the associated eigenvectors. Note that e_i are orthonormal vectors. Then

$$\hat{\Phi}^{-1} = \sum_{i=1}^{M+1} \frac{e_i e_i^{\dagger}}{\lambda_i} \quad . \tag{3}$$

Let λ_1 be the largest eigenvalue and λ_{M+1} be the smallest eigenvalue of $\hat{\Phi}$, then (3) can be written as

$$\hat{\Phi}^{-1} = \frac{1}{\lambda_{M+1}} \left[I - \sum_{i=1}^{M} \frac{\lambda_i - \lambda_{M+1}}{\lambda_i} e_i e_i^{\dagger} \right]. \tag{4}$$

In (4), we have made use of the fact that

$$\sum_{i=1}^{M+1} e_i e_i^{\dagger} = I \tag{5}$$

8

where I is an identity matrix. Using (4) in (1), one gets

$$W = \mu' \left[S - \sum_{i=1}^{M} \frac{\lambda_i - \lambda_{M+1}}{\lambda_i} e_i \alpha_i \right] \qquad (6)$$

where

$$\mu' = \frac{\mu}{\lambda_{M+1}}$$

and

$$\alpha_i = e_i^{\dagger} S .$$

Equation (6) shows that W consists of two parts: the first part is the steering vector S; the second part, which is subtracted from S, is the summation of weighted orthogonal eigenvectors. The eigenvectors are multiplied by a factor involving the eigenvalues of the covariance matrix, $\hat{\Phi}$.

For source distributions which involve a small number of available degrees of freedom (the number of array elements is larger than the number of signals incident on the array), the eigenvalues λ_i can be divided into two groups: the unique eigenvalues generated by the spatial source distribution and noise eigenvalues generated by the thermal noise in various antennas. The unique eigenvalues depend on the spatial distribution of the signal sources and their signal strengths while noise eigenvalues are approximately equal to the thermal noise

9

power, σ^2, in the array elements. The eigenvectors corresponding to the unique eigenvalues affect the weights of the adaptive array. For example, if the signal scenario consists of a single CW signal of amplitude A and the adaptive array is an array of M+1 isotropic elements then the eigenvalues of the covariance matrix, $\hat{\Phi}$, are [10]

$$\lambda_i = \begin{cases} (M+1)A^2 + \sigma^2 & i=1 \\ \sigma^2 & i=2,3,\ldots M+1 \end{cases} \quad (7)$$

and from (6)

$$W = \frac{\mu}{\sigma^2} \left[S - \frac{(M+1)A^2}{(M+1)A^2+\sigma^2} e_1\alpha_1 \right]$$

$$= \frac{\mu}{\sigma^2} \left[S - \frac{1}{1 + \frac{\sigma^2}{(M+1)A^2}} e_1\alpha_1 \right] . \quad (8)$$

For weak signals, $\frac{A^2}{\sigma^2} \ll 1$, (8) can be approximated as

$$W \simeq \frac{\mu}{\sigma^2} S. \quad (9)$$

Thus, the weight vector will be proportional to the steering vector and the output SNR of the adaptive array will be the same as that in the quiescent state. In the case of an interfering signal this means that the interference will not be suppressed. Now, let us modify the covariance matrix, $\hat{\Phi}$, such that

10

$$\Phi = \hat{\Phi} - F\lambda_{m+1} I \tag{10}$$

where F is a constant and can have values between 0 and 1. Note that Φ is obtained from $\hat{\Phi}$ by subtracting a fraction, F, of its smallest eigenvalue from the diagonal terms. Then e_i, $i=1,2,...M+1$ are the orthonormal eigenvectors of Φ and its eigenvalues are $\lambda_i - F\lambda_{M+1}$. If Φ instead of $\hat{\Phi}$ is used to compute the adaptive array weights then

$$W = \frac{\mu'}{1-F}\left[S - \sum_{i=1}^{M} \frac{\lambda_i - \lambda_{M+1}}{\lambda_i - F\lambda_{M+1}} e_i \alpha_i \right]. \tag{11}$$

Again, W consists of two parts: the first part is the steering vector S; the second part, which is subtracted from S, is the summation of weighted orthogonal eigenvectors. However, the factor with which eigenvectors are multiplied has changed. Now, the eigenvectors are multiplied by a factor $\dfrac{\lambda_i - \lambda_{M+1}}{\lambda_i - F\lambda_{M+1}}$ instead of $\dfrac{\lambda_i - \lambda_{M+1}}{\lambda_i}$. This change in the multiplying factor, as shown below, helps in suppressing weak interfering signals. Let us again consider the case of a single signal scenario. Then using (7) in (1), one gets

$$W = \frac{\mu}{(1-F)\sigma^2}\left[S - \frac{1}{1 + \dfrac{1-F}{M+1}\dfrac{\sigma^2}{A^2}} e_1 \alpha_1 \right] \tag{12}$$

Now for weak interfering signals, $\dfrac{A^2}{\sigma^2} \ll 1$, one can adjust F such that $\dfrac{1-F}{M+1}\dfrac{\sigma^2}{A^2} \ll 1$. Then from (12),

11

$$W \simeq \frac{\mu}{(1-F)\sigma^2} \left[S - e_1 \alpha_1 \right].$$
(13)

Thus, the array will adjust its weights according to the signal scenario, irrespective of the signal strength. In the case of an interfering signal, the weights will be adjusted to suppress the interfering signal.

Figure 4 shows the output INR of the 4-auxiliary element adaptive array versus the fraction F. The input INR in the main antenna is -5 dB while all other parameters are the same as in Figure 3. Curves for various values of the auxiliary antenna gains (G_a) in the interference signal direction are given. The input INR in each auxiliary antenna is equal to the gain of the auxiliary antenna minus 13 dB. Note that the output INR decreases with an increase in F. Thus, by increasing the fraction (F) of the smallest eigenvalue subtracted from the diagonal elements of the sample covariance matrix, $\hat{\Phi}$, one can increase the interference suppression. However, as F approaches unity, one may face numerical problems in the inversion of the matrix $\hat{\Phi}$. This should be kept in mind while selecting F.

An important observation to be made from the plots in Figure 4 is that one can trade off the gain of the auxiliary antennas with the fraction, F, i.e., one can decrease the auxiliary antenna gain and increase F or vice versa to achieve a specified interference suppression. For example, for a 20 dB interference suppression (output INR would be approximately -25 dB), F for isotropic auxiliary antennas is 0.98 while for 6 dB and 10 dB auxiliary antennas, F, respectively, is 0.90 and 0.76. Thus, the larger the auxiliary antenna gain, the smaller

12

the fraction F to achieve a specified interference suppression. The output SINR of the adaptive array is studied next to find a trade off between these two quantities.

IV. OUTPUT SINR

Figure 5 shows the output SINR of the 4-auxiliary element adaptive array versus the fraction F for various auxiliary antennas. All parameters are the same as in Figure 4. Note that for highly directive auxiliary antennas ($G_a \geq 10$ dB), the output SINR does not change much with F. The output SINR is approximately equal to the input SNR in the main channel. Thus, highly directive auxiliary antennas suppress the undesired signal without adversely affecting the SNR. This is not true for low gain ($G_a < 10$ dB) auxiliary antennas. For low gain auxiliary antennas, the output SINR is less than the input SNR in the main antenna (14.6 dB) and the output SINR degrades with an increase in F. The degradation in the output SINR is due to the following reason.

The thermal noise in the auxiliary antennas is uncorrelated with the thermal noise in the main antenna. Therefore, whenever the auxiliary antennas are activated, additional thermal noise appears at the output port resulting in SINR degradation. The amount of thermal noise added by the auxiliary antennas depends on the magnitude of the auxiliary antenna weights. The larger the weights, the larger the thermal noise added by the auxiliary antennas. The weights of the auxiliary antennas depend on the relative amplitude of the interfering signal in the auxiliary antennas compared to the interfering signal in

13

the main antenna[*]. If the interfering signal in the auxiliary antennas is weaker than the interfering signal in the main antenna (low gain auxiliary antennas), the weights will be large (assuming that the interference is being cancelled) and consequently the auxiliary antennas will add more noise to the array output. On the other hand, if the interfering signal in the auxiliary antennas is stronger than the interfering signal in the main antenna (auxiliary antennas have high gain), the weights will be small and consequently less noise will be added to the array output. Thus, for low gain auxiliary antennas, the output SINR is smaller than the input SNR in the main antenna. In the case of low gain auxiliary antennas, one needs a large F to achieve the desired interference suppression (see Figure 4). Thus, interference suppression is accompanied by a drop in the output SINR. To avoid this SINR degradation, the auxiliary antennas should be selected such that the interfering signal amplitude in the auxiliary antennas is at least equal to the interfering signal in the main antenna. Then the fraction F should be adjusted to achieve the required interference suppression.

V. DEFOCUSED FEED AS AUXILIARY ELEMENTS

In the last section it was shown that for better performance, the auxiliary elements of a modified SMI adaptive array should be directive

---

* The desired signal level in the auxiliaries is very small as compared to that in the main antenna and the components of the steering vector are proportioned to the desired signal level in the corresponding antenna elemenets. Thus, in the presence of the desired signal only, the auxiliary elements weights will be very small.

and should be pointed in the general direction of the interfering signal
sources. In the case of reflector antenna, by moving the feed away from
the focus, one can steer the beam of the antenna over a wide angular
region. Thus, by a proper selection of the feed location, one can steer
the main beam in the general direction of an interfering signal and by
using an array of feeds, all signals (desired and undesired) can be
received with high gain. In this section, the performance of the
modified SMI adaptive array is studied when the defocused feeds of the
reflector antenna (the main antenna) are used as auxiliary elements.
The description of the main antenna is given below.

A. The Main Antenna and its Radiation Characteristics

The main antenna, shown in Figure 6, is a 4.5 meter center-fed,
vertically polarized (along y axis) circular reflector with an F/D radio
of 0.5. The frequency of operation is 4 GHz. At this frequency, the
maximum gain of the antenna is 45.5 dB and its half power beam width
(HPBW) is approximately 1.9°. Since we plan to use defocused feeds of
this reflector as auxiliary elements of the adaptive arrays, its
radiation pattern for various feed locations were computed. The Ohio
State University ElectroScience Laboratory's NEC – Reflector Antenna
Code [11,12] was used for this purpose. A description of the code and
the radiation patterns of the reflector antenna for various feed
locations are given below.

The NEC – Reflector Antenna Code can be used to compute the near-
field as well as the far-field of a reflector antenna with a
paraboloidal surface. The code utilizes a combination of the

Geometrical Theory of Diffraction (GTD) and Aperture Integration (AI) techniques to compute the antenna pattern. Typically, AI is used to compute the far-field main beam and first sidelobes while GTD is used to compute the wide angle sidelobes and backlobes. For near-field calculations, GTD is used for the whole region. The code can be used to include spillover, feed blockage and scattering from struts, etc., and to compute the antenna pattern when the feed is not at the focus (defocused feed or offset feed) of the reflector.

To compute the antenna pattern, the feed pattern should be specified. In the code, the feed pattern can be specified by piecewise linear feed data or an analytic function. In the case of a horn feed, one need only specify the horn dimensions. The code then computes the feed pattern. The analytic function used to define the feed pattern is

$$F(\psi) = \frac{\exp\left(-A \left(\frac{\psi}{\psi_o}\right)^2\right) \left[\cos^N\left(\frac{\pi\psi}{2\psi_o}\right) + c\right]}{1 + c} \qquad (14)$$

where the constants A, ψ_o, N and c can be controlled for each feed pattern cut ϕ_n (Figure 7). The constants A, c and N control the shape of the feed pattern while ψ_o permits a given pattern shape to be stretched or compressed. For large values of $\frac{\psi}{\psi_o}$ (>1), $F(\psi) \rightarrow \frac{c}{1+c}$. In many cases, this represents a spillover level that is too high for typical feed patterns. Consequently, under certain conditions, a linear taper, as shown in Figure 8, is used for $\psi_L < \psi < 2\psi_L$ where

$$\psi_L = \sqrt{\frac{3}{A}} \; \psi_0 \; . \tag{15}$$

The linear taper is found to give reasonable results for $N=1$, $C \geq 0$ and $A > 3$. Otherwise, Equation (14) is used for the entire feed pattern.

In this study, an analytic function is used to specify the feed pattern. The feed pattern is assumed to be circularly symmetric (independent of ϕ_n). The constants A, c and N are chosen to be 3.1, 0. and 1, respectively. This choice leads to a cosine aperture illumination and a small spillover. ψ_0 is chosen such that the edge illumination is -10 dB. Figure 9 shows the feed pattern in the y-z plane ($\phi_n = 90°$). Note that the edge illumination is -10 dB (edge angle is 53°) and a linear taper is used for $\psi > \psi_0$, where $\psi_0 = 106°$.

Figure 10 shows the far-field pattern of the reflector in the y-z plane ($\phi = 90°$) for $-30° \leq \theta \leq 30°$ when the feed is assumed to be at the focus of the reflector. Since we are interested in the general shape of the radiation pattern, aperture blockage and scattering from struts are not included to save computational time. The plot shows the gain of the antenna (over an isotropic radiator) in various directions. The main beam of the antenna is along the z axis ($\theta = 0°$) and its gain in this direction is 44.5 dB which is within a dB of the maximum gain of the antenna. The first sidelobe level is 17 dB (27.5 below the main beam). Thus, the SNR of a signal entering the sidelobes will be much lower than that of a signal entering the main beam, even though the EIRP of the two signals is approximately the same.

17

Figure 11 shows the radiation pattern of the antenna when the feed is moved one wavelength away from the focus along the positive y axis. All other parameters are the same as before. Note that the main beam of the antenna has moved to $-2.5°$. The gain of the antenna in this direction is 44.37 dB. Thus, a signal incident from this direction will have a high SNR at the output of this feed while its SNR at the output of the feed at the focus will be quite low. Figures 12 and 13 show the radiation patterns of the antenna when the feed is moved two and three wavelengths, respectively, away from the focus along the positive y axis. Note that the main beam of the antenna moves further away from the z axis ($\theta = 0°$) and the maximum gain of the antenna is within one dB of its value when the feed is at the focus (Figure 10). Thus, the feeds at these locations can be used very effectively to receive signals incident from angles corresponding to the sidelobes of the center-fed antenna.

Figure 14 and 15 show the radiation pattern of the antenna when the feed is moved two and three wavelengths, respectively away from the focus along the negative y axis. All other parameters are the same as in Figure 10. Note that the main beam of the antenna moves along the positive θ direction and its maximum gain is more or less unchanged. Thus, by moving the feed away from the focus along the y axis one can steer the main beam of the antenna over a wide angular region in the y-z plane. Similarly, by moving the feed along the x axis, the main beam can be steered in the x-z plane. Therefore, by moving the feed away from the focus of a reflector antenna, one can steer the main beam over a wide angular region without any significant loss of signal strength

18

and by using an array of feeds, all signals (desired or undesired) incident on the antenna can be received with high gain, provided that the angles of arrival of the various signals are known approximately.

In the last section, we had shown that by using directive auxiliary antennas in SMI adaptive arrays, one can suppress weak interfering signals. Thus, when the main antenna is a reflector antenna, one can use defocused feeds as auxiliary antennas to suppress weak interfering signals. The performance of such an SMI adaptive antenna array is studied next.

B. Performance in an Adaptive Mode

In the communication systems under consideration, the satellites are located in geosynchronous orbits. Thus, interfering signal sources are nearly coplanar with the desired signal source. In this work, all signals (desired and undesired) are assumed to be in the y-z plane (Figure 16). The desired signal is incident along the z axis ($\theta = 0°$) and to facilitate its reception one feed is located at the focus of the reflector antenna. The desired signal intensity is assumed to be such that the SNR at an isotropic antenna is -30 dB. The gain of the reflector antenna in the desired signal direction is 44.51 dB (Figure 10). Thus, the SNR at the output of the feed at the focus is approximately 14.5 dB. This feed will also receive some undesired signals through the sidelobes of the reflector antenna. The interfering signals are assumed to be coherent and similar in nature to the desired signals.

19

Figure 17 shows the interference-to-noise ratio (INR) at the output of the feed at the focus when the signal scenario consists of a single interfering signal. The EIRP of the interfering signal is the same as that of the desired signal, i.e., the INR at an isotropic antenna is -30 dB. This case corresponds to the situation where the interference is caused by a satellite serving the same geographical area. The output INR is plotted vs. the interfering signal direction. Note that the INR is very low. In fact, the interfering signal is below the noise level by several dB (maximum output INR is -10 dB). However, this signal because of its coherent nature and its similarity to the desired signal, does cause objectionable interference and must be further suppressed.

Figure 18 shows the output INR when an additional feed (defocused feed) is used and the signals received by the two feeds are weighted adaptively. Modified SMI algorithm is used to compute the two weights. The additional feed is located two wavelengths away from the focus along the positive y axis. In Figure 18, the output INR is plotted for three values (0., 0.04, 0.8) of the factor F. Comparing the plots in Figure 17 and 18, one can see that for F=0 (conventional SMI), the interference is suppressed significantly if its angle of arrival is between -4.6° and -2.6°. The main beam of the reflector with the additional feed is in this angular region. Thus a conventional SMI adaptive antenna can provide the required interference suppression if the auxiliary antenna is highly directive and is steered in the interference signal direction. However, this may not be feasible in practice (interference direction is not known exactly).

20

For other values of F (modified SMI), the interference suppression is quite small. Actually for F=0.8, the output INR is more than the INR in the main feed. This is in contradiction with out earlier observation (see Section III). The reason for this discrepancy is that the number of signals incident on the adaptive array is equal to the number of antenna elements in the array. Thus, the smallest eigenvalue of the covariance matrix does not correspond to the noise eigenvalue and the modified SMI algorithm can not be used.

Figure 19 shows the output INR when two defocused feed are used and the signals received by the three feeds are adaptively weighted and then summed to form the array output. All other parameters are the same as before. The second defocused feed is located three wavelengths away from the focus along the positive y axis. Note that, as expected, the interference suppression and the angular region in which the interference is suppressed increases with an increase in F. Comparing the plots in Figures 19 and 21, one can see that even for F=0 (conventional SMI), the interference is suppressed significantly if its angle of arrival is between -6.5° and -2.6°. The two defocused feeds have their main beams in this angular region.

Figure 20 shows the output SINR of the adaptive array. The output SINR is approximately 14.5 dB for all angels of arrival of the interference signal. Thus, the interference is suppressed without adversely affecting the desired signal or SNR. Hence defocused feeds of a reflector can be used as auxiliary elements of an SMI adaptive array provided that the interference signal source direction is approximately known and the defocused feeds are located to steer the main beam of the

21

reflector antenna in that general direction. Further, if the modified SMI algorithm is used, the total number of feeds should be more than the number of signals incident on the array.

Figure 21 shows the INR at the output of the feed at the focus of the reflector when the signal scenario consists of a desired signal and two interfering signals. The desired signal parameters are the same as before. The EIRP of the interfering signals are assumed to be such that the INR of each interfering signal at an isotropic antenna is -30 dB. One of the interfering signals is fixed and its angle of arrival is -5.5° (in the y-z plane) while the other interfering signal is swept between -10° and -2°. The output INR is plotted versus the second interfering signal's direction. Comparing the INR in this figure with that in Figure 17, one can see that the INR in the presence of two interfering signals is significantly higher than that in the presence of one interfering signal. The reason for this is that the fixed interfering signal is incident at the peak of a sidelobe of the center-fed reflector.

Figure 22 shows the output INR of the three element adaptive array (two defocused feeds at 2λ and 3λ spacing are used). All parameters are the same as in Figure 21. The output INR is plotted for various values of F. Note that for F=0, whenever the angle of arrival of the swept interference is between -6° and -5.2° or -4.5° and -2.6°, the output INR of the array is significantly lower than the INR in the main channel (Figure 21). With the two defocused feeds, the main beam of the reflector is in these angular regions. Thus, using two defocused feeds, both interfering signals can be suppressed provided that the angular

22

regions of the interference signals are covered by the two feeds. The interference suppression in the angular region -4.5° and -2.6° decreases with an increase in the value of F. As pointed out before, this is because the array does not have enough degrees of freedom (total number of signals incident on the array is equal to the total number of array elements). The increase in the interference suppression in the angular region -6° to -5.2° with an increase in F is due to the reason that the two interfering signals are incident from the same direction and thus only one degree of freedom is required to null both interfering signals.

Figure 23 shows the output INR of the adaptive array when another defocused feed is added. The new defocused feed is located at (0., -3λ, 0.) with respect to the focus. With this defocused feed, the reflector has its main beam along 5.5° in the y-z plane (see Figure 15). Note that now, as expected, the output INR decreases with an increase in the value of F. The angular region in which the interference is suppressed also increases with F. Thus, the modified SMI adaptive array (F≠0) performs better than the conventional adaptive array (F=0). However, one needs an extra degree of freedom to implement the modified SMI algorithm.

Figure 24 shows the output SINR of the four element adaptive array. All parameters are the same as in Figure 23. Note that for all values of F, the output SINR for all angles of arrival of the interfering signal is approximately 14.5 dB, which is equal to the SNR at the output of the main antenna (feed at the focus). Thus, the interference are suppressed without any degradation in the SNR. Hence the defocused feeds of a reflector antenna can be very effectively used to suppress

23

weak interfering signals provided that the angular region from which the interfering signal arrive are covered by the beams obtained using the defocused feeds. Further, for the best performance, the number of degrees of freedom of an SMI adaptive array should be more than the total signals incident on the array. Some general conclusions of the study are given below.

V. CONCLUSIONS

Conventional adaptive antenna arrays are unable to suppress weak interfering signals (INR $\leq$ -5 dB). The reason for the lack of interference suppression is that for weak interfering signals, the thermal noise is the main source of degradation in the output SINR and thus it (thermal noise) dictates the array weights. An adaptive array adjusts its weights to minimize the thermal noise which in turn maximizes the output SINR. However, the interference remains unsuppressed. To overcome this difficulty, the SMI algorithm used to compute the array weights was modified. In the modified algorithm, the covariance matrix is modified so that the effect of thermal noise on the weights of an adaptive array is reduced. It was shown that the modified SMI algorithm provides the required interference suppression without adversely affecting the output SINR even when the auxiliary antennas are moderately directive. Further, it was shown that when the main antenna is a reflector antenna, one can use defocused feeds as auxiliary elements of a modified SMI adaptive array.

In this report, covariance matrix, Φ, was assumed to be known exactly. In practice, the covariance matrix is computed using a finite

24

number of snapshots. In the presence of weak interfering signals, one may need a large number of snapshots to get a good estimate of the covariance matrix. In the satellite communication systems under consideration, the satellites are in geosynchronous orbits. Thus, the signal scenario does not change too fast and one can use a large number of snapshots without a performance penalty. For other communication systems, the number of snapshots required to get a good estimate of the covariance matrix should be found.

A problem which one may have to face in the implementation of the proposed algorithm is the inversion of the covariance matrix Φ (Equation (10)). The covariance matrix Φ is obtained by subtracting a constant from each of the diagonal terms of the sample matrix, $\hat{\Phi}$. This makes Φ more ill conditioned. One can avoid this problem by writing

$$\Phi^{-1} = \sum_{i=1}^{M+1} \frac{e_i \, e_i^{\dagger}}{\lambda_i - F\lambda_{M+1}} \tag{16}$$

where λ_i, $i=1,2,\ldots M+1$ are the eigenvalues of $\hat{\Phi}$ with e_i, $i=1,2,\ldots M+1$ the associated eigenvectors. One might have computed these quantities while computing the smallest eigenvalues of $\hat{\Phi}$. Thus Φ^{-1} can be computed without any problem.
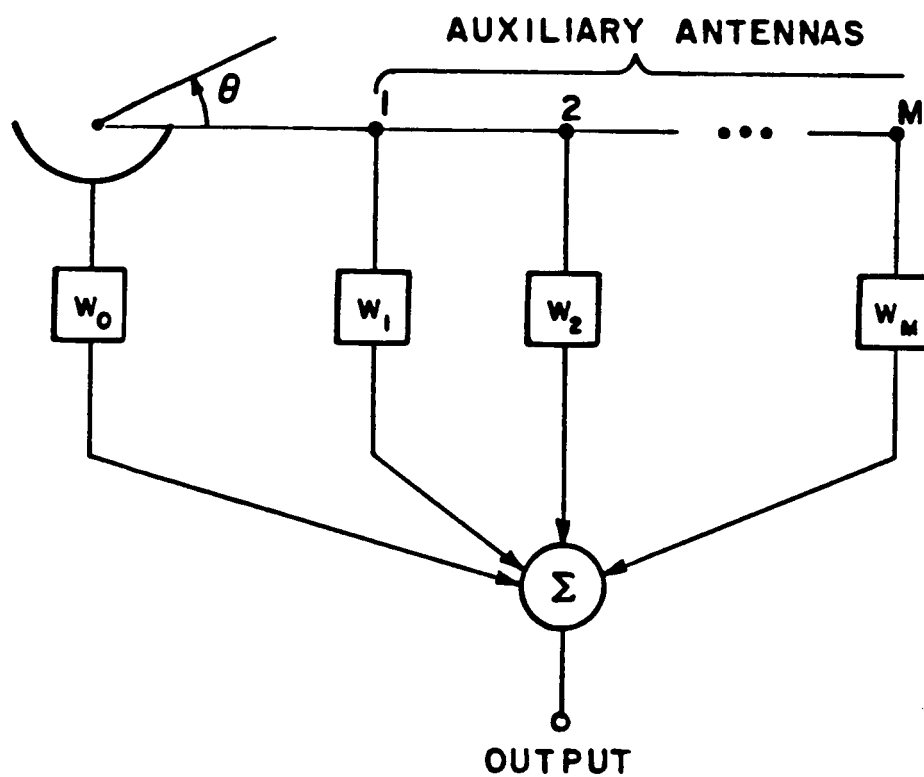
Figure 1. Schematic of an adaptive array.
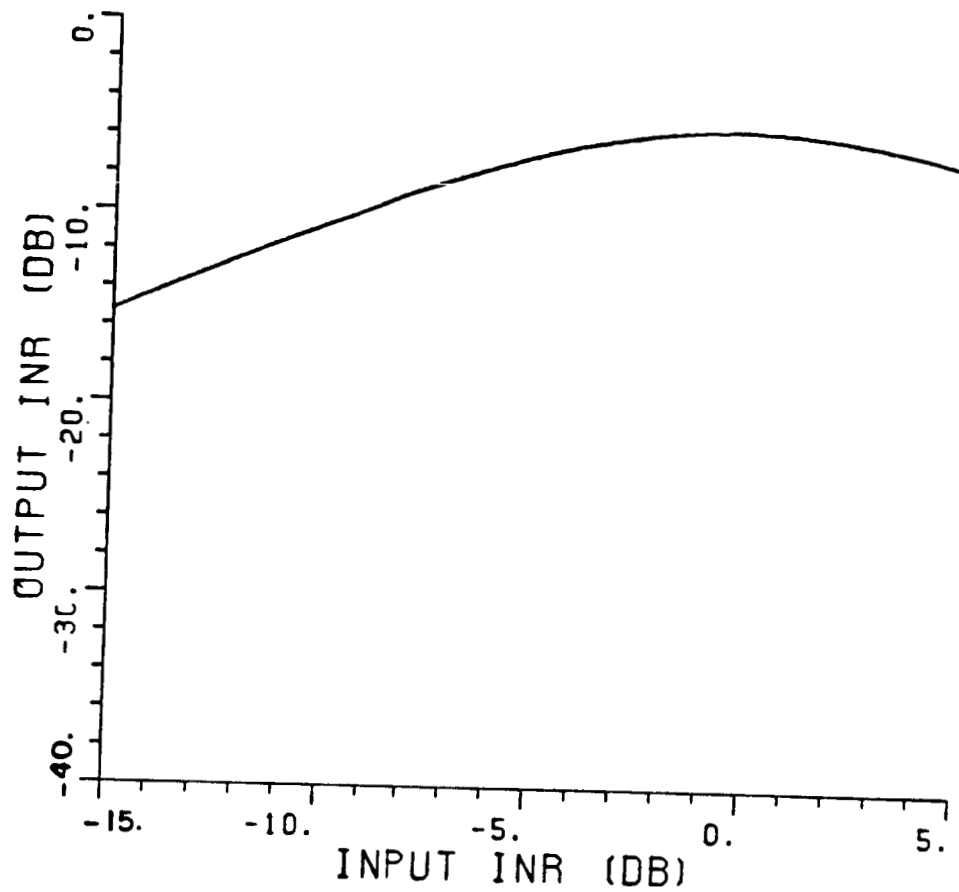
SNR (main) = 14.6 dB

SNR (aux) = -10 dB,

$\theta_d = 90°$, $\theta_i = 60°$

INR (aux) = INR (main) - 8 dB.

Figure 2.   Output INR of a 4-auxiliary element SMI adaptive array vs. the input INR in the main antenna.

27
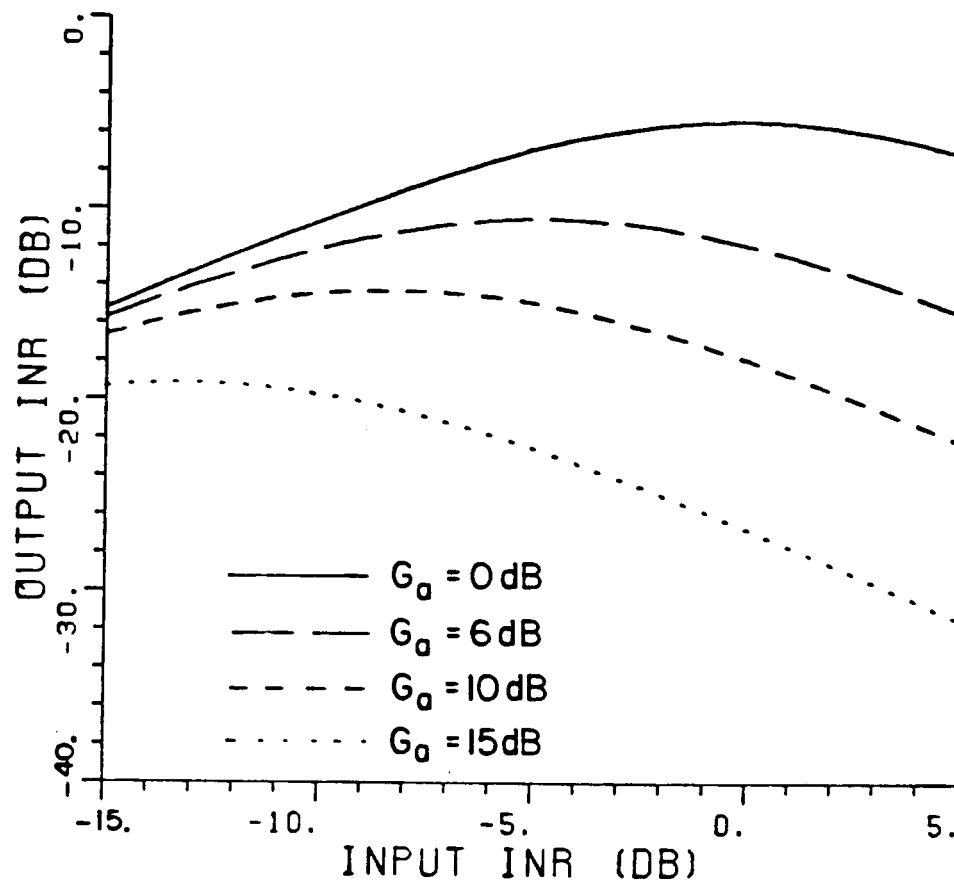
SNR (main) = 14.6 dB

SNR (aux) = -10 dB,

$\theta_d = 90°$, $\theta_i = 60°$

INR (aux) = INR (main) + G_a - 8 dB

Figure 3. Output INR of a 4-auxiliary element adaptive array vs. the input INR in the main antennas for various gain auxiliary antennas.

28
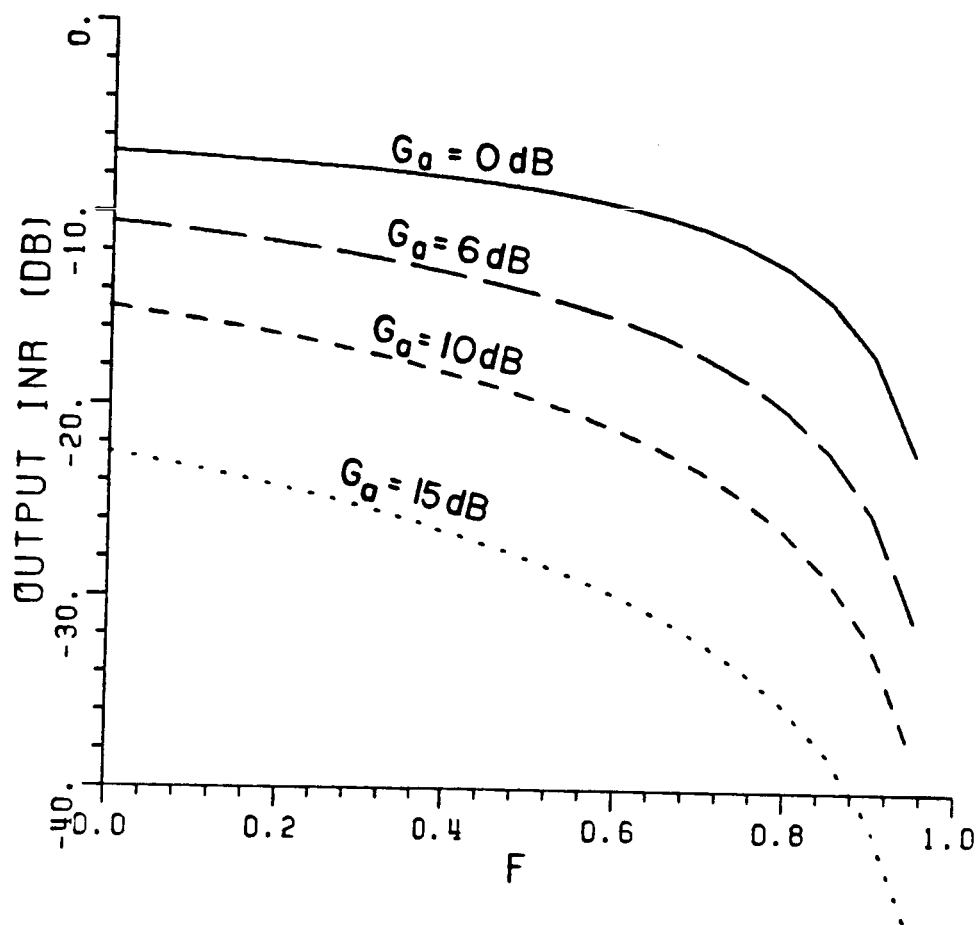
SNR (main) = 14.6 dB

SNR (aux) = -10 dB

INR (main) = -5 dB

INR (aux) = G_a - 13 dB

$\theta_d = 90°$, $\theta_i = 60°$

Figure 4. Output INR of a 4-auxiliary element adaptive array vs. the fraction F for various gain auxiliary antennas.

29
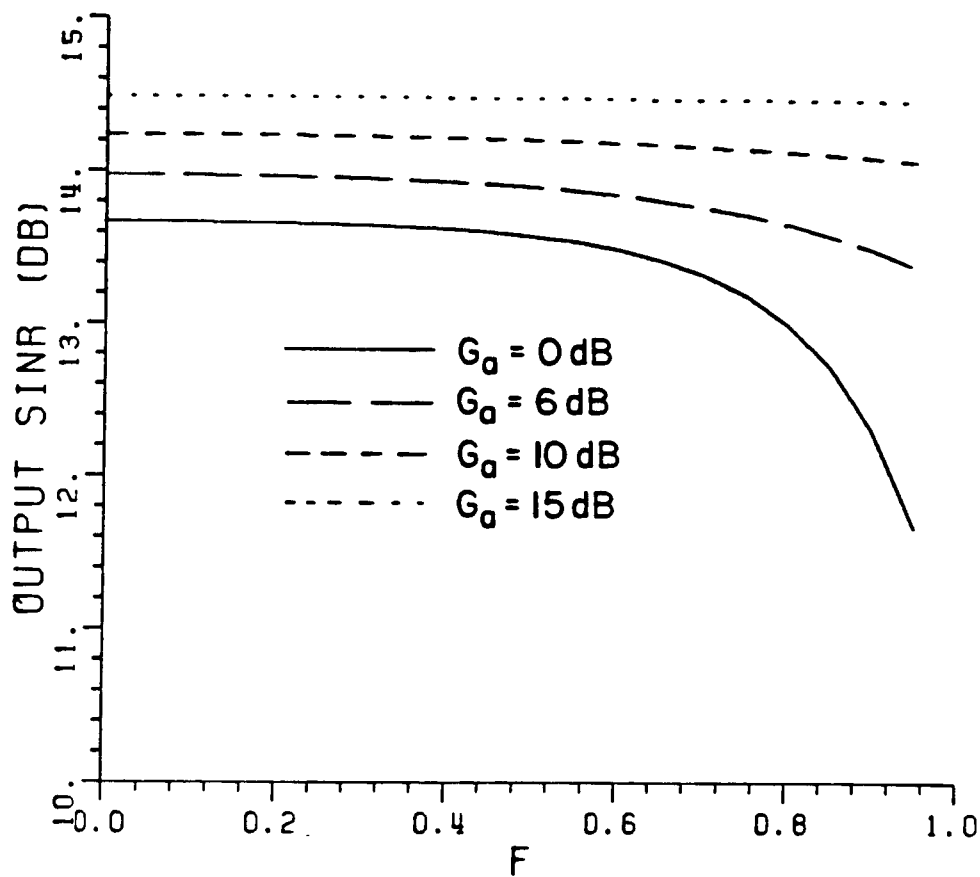
Figure 5. Output SINR of a 4-auxiliary element adaptive array vs. the fraction F for various gain auxiliary antennas.

SNR (main) = 14.6 dB

SNR (aux) = -10 dB

INR (main) = -5 dB

INR (aux) = G_a - 13 dB

$\theta_d = 90°$, $\theta_i = 60°$
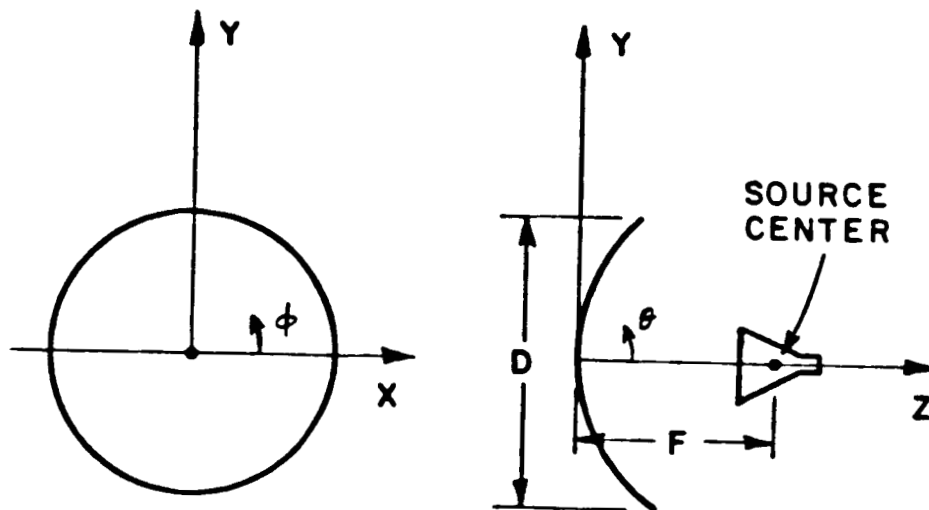
Figure 6.   Center-fed circular reflector.

31
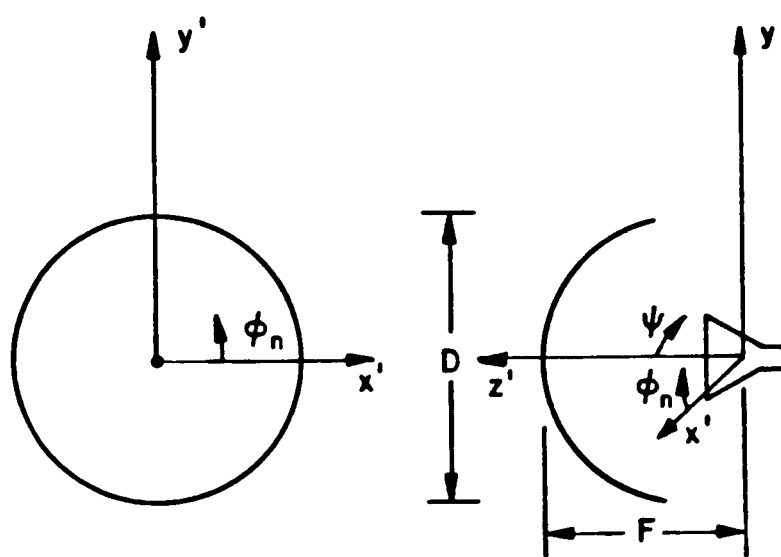
Figure 7. Center-fed circular reflector.
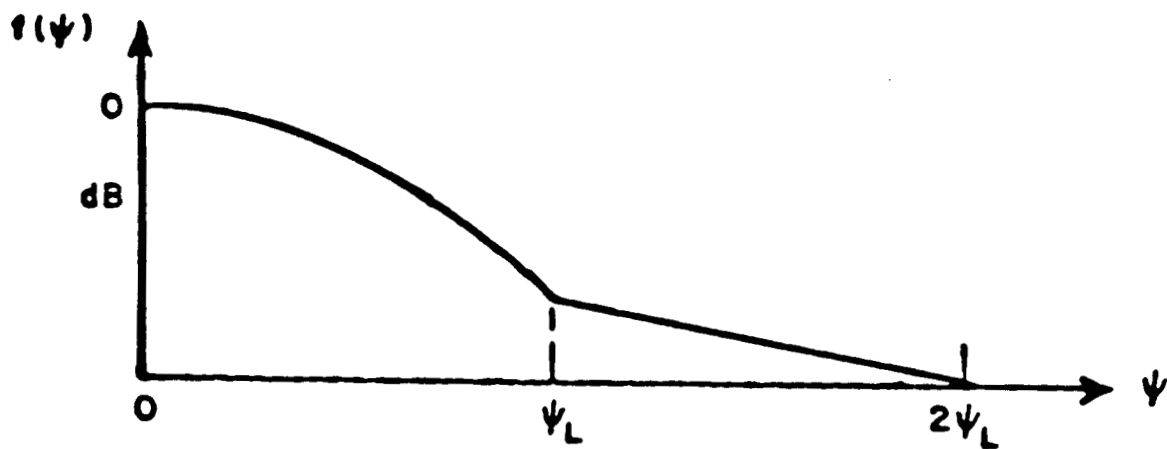
Figure 8.   Analytic feed pattern with linear taper design.
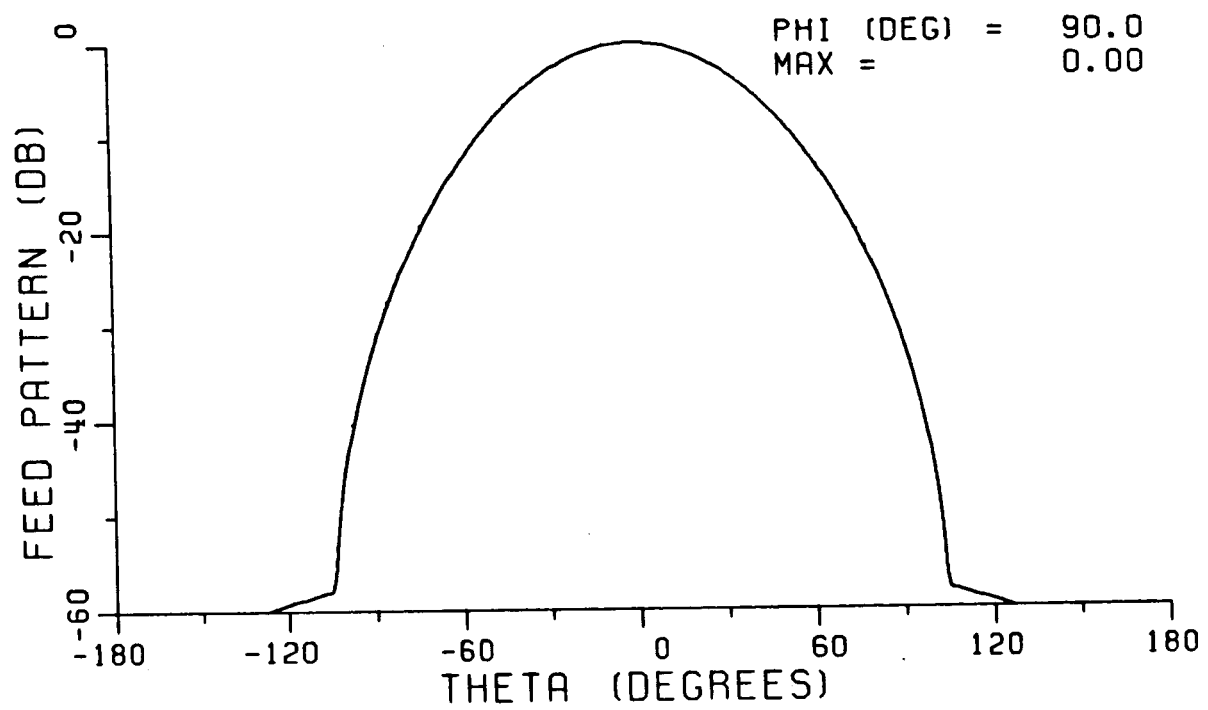
Figure 9. Feed pattern in the y-z plane.

PHI (DEG) =   90.0
F   (WL)   =   30.0
D   (WL)   =   60.00
MAX   =   44.51
AI   GTD   SPILLOVER
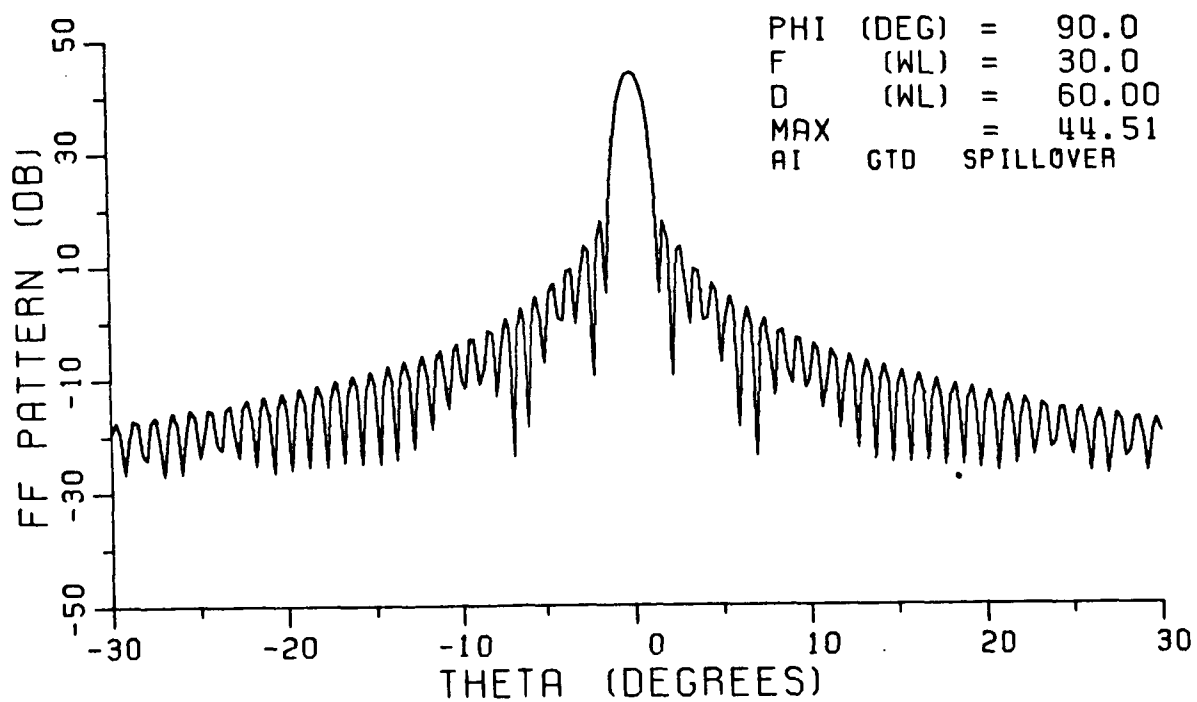
Figure 10. Radiation pattern of the antenna in the y-z plane when the
feed is at the focus.

35
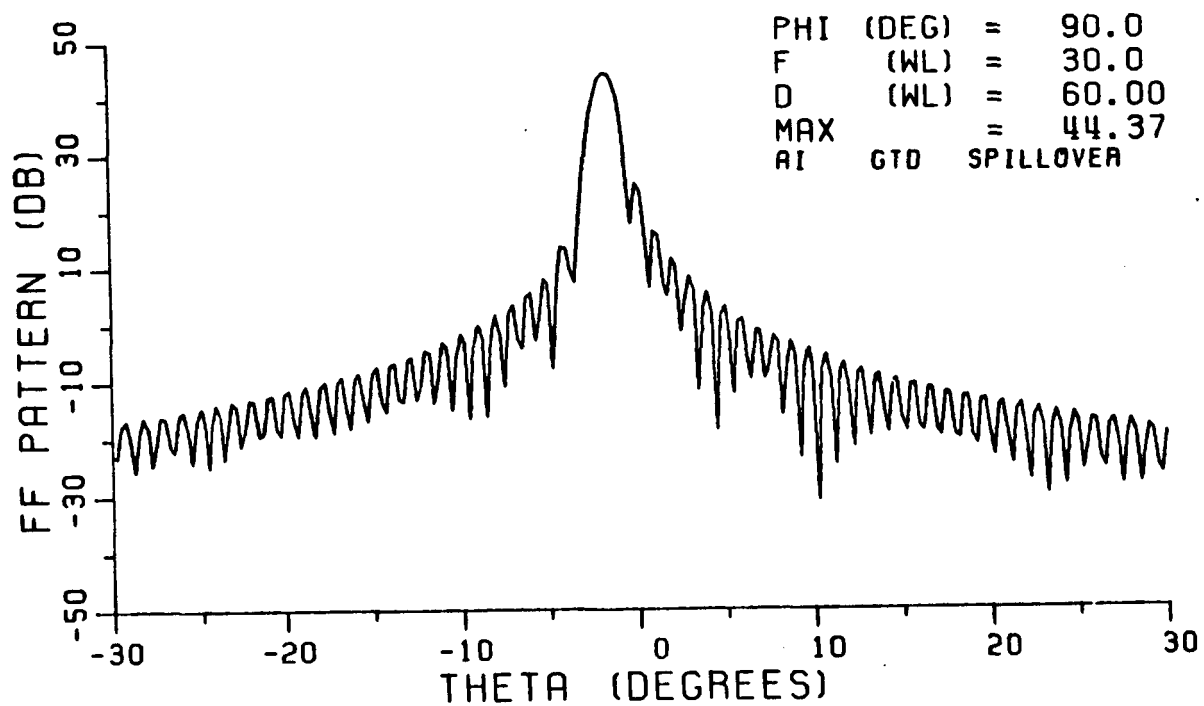
Figure 11. Radiation pattern of the antenna in the y-z plane when the feed is (0., λ, 0.) away from the focus.

PHI (DEG) = 90.0
F (WL) = 30.0
D (WL) = 60.00
MAX = 44.08
AI GTD SPILLOVER

FF PATTERN (DB)

THETA (DEGREES)
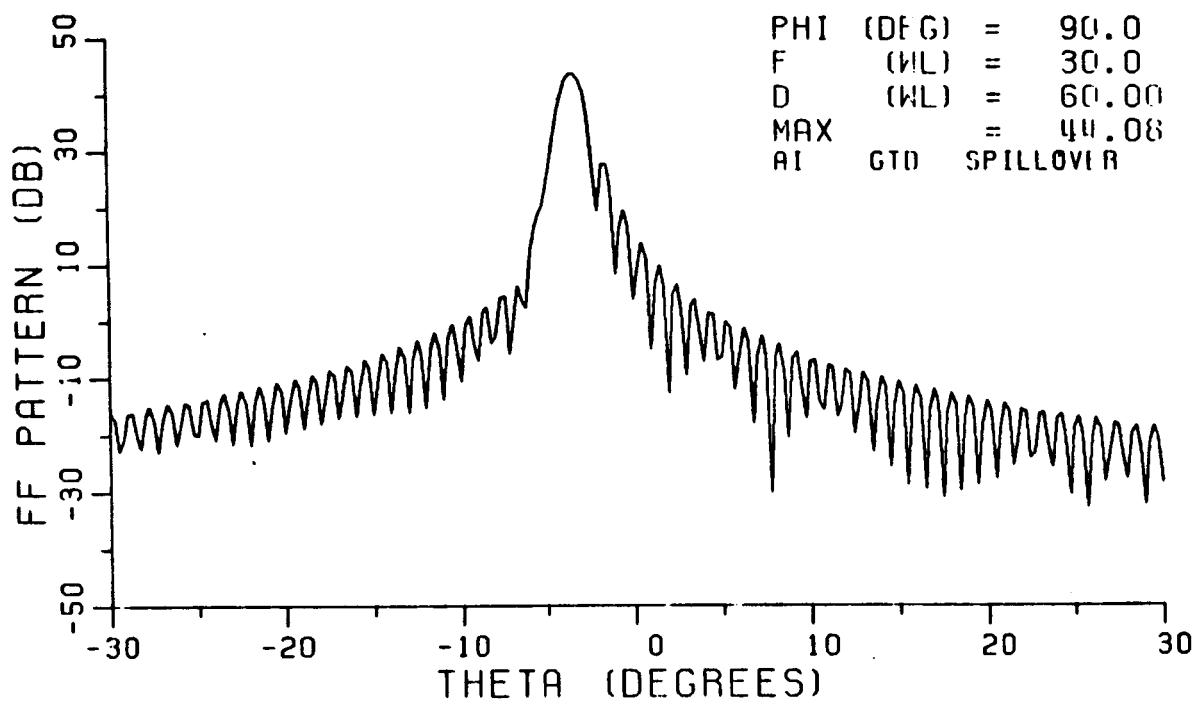
Figure 12. Radiation pattern of the antenna in the y-z plane when the feed is (0., 2λ, 0.) away from the focus.

37
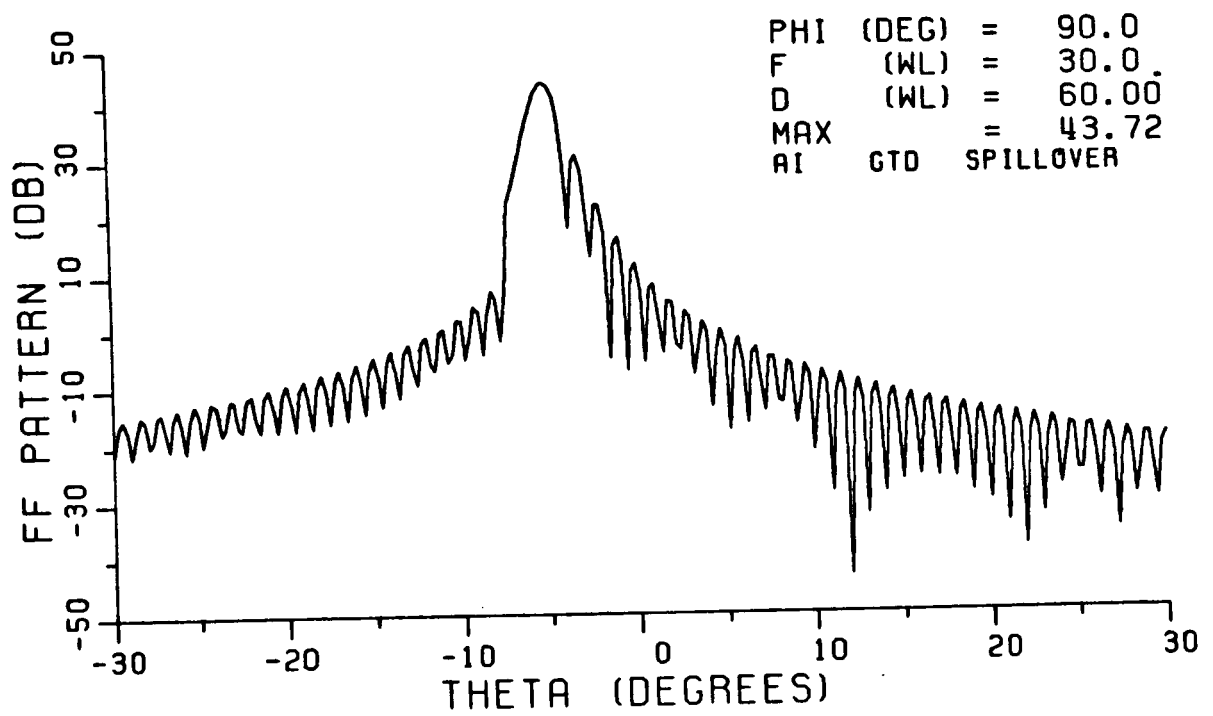
Figure 13. Radiation pattern of the antenna in the y-z plane when the feed is (0., 3λ, 0.) away from the focus.
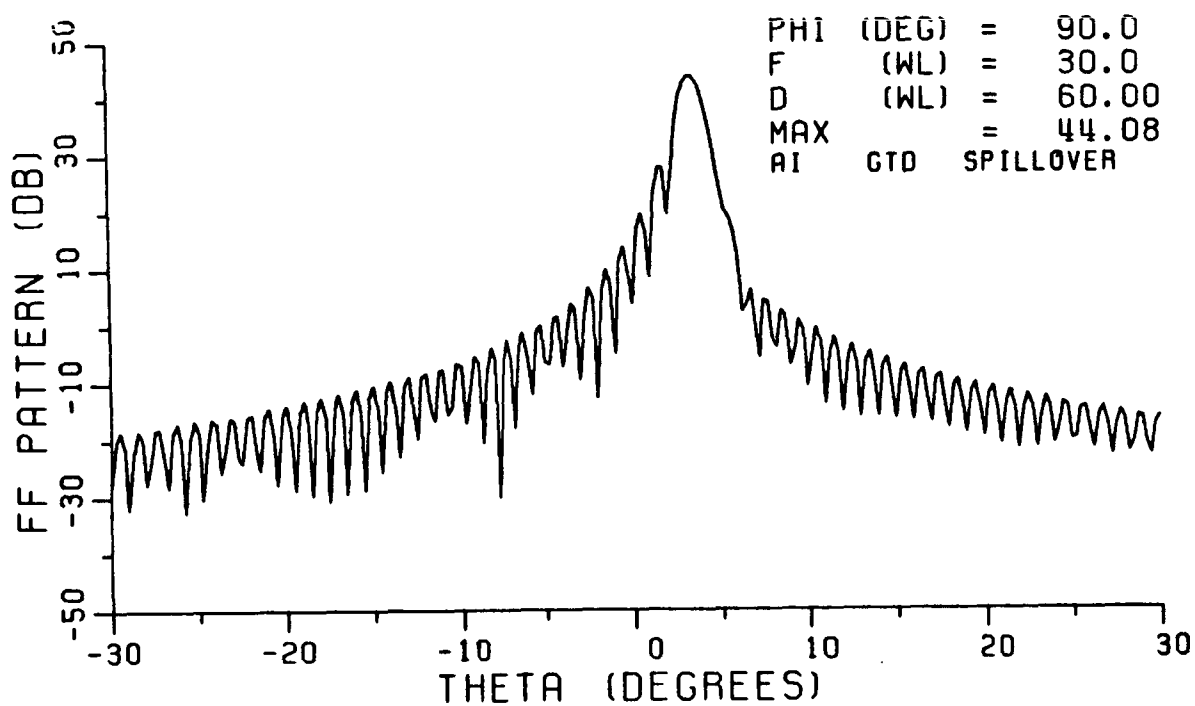
Figure 14. Radiation pattern of the antenna in the y-z plane when the feed is (0., -2λ, 0.) away from the focus.

39
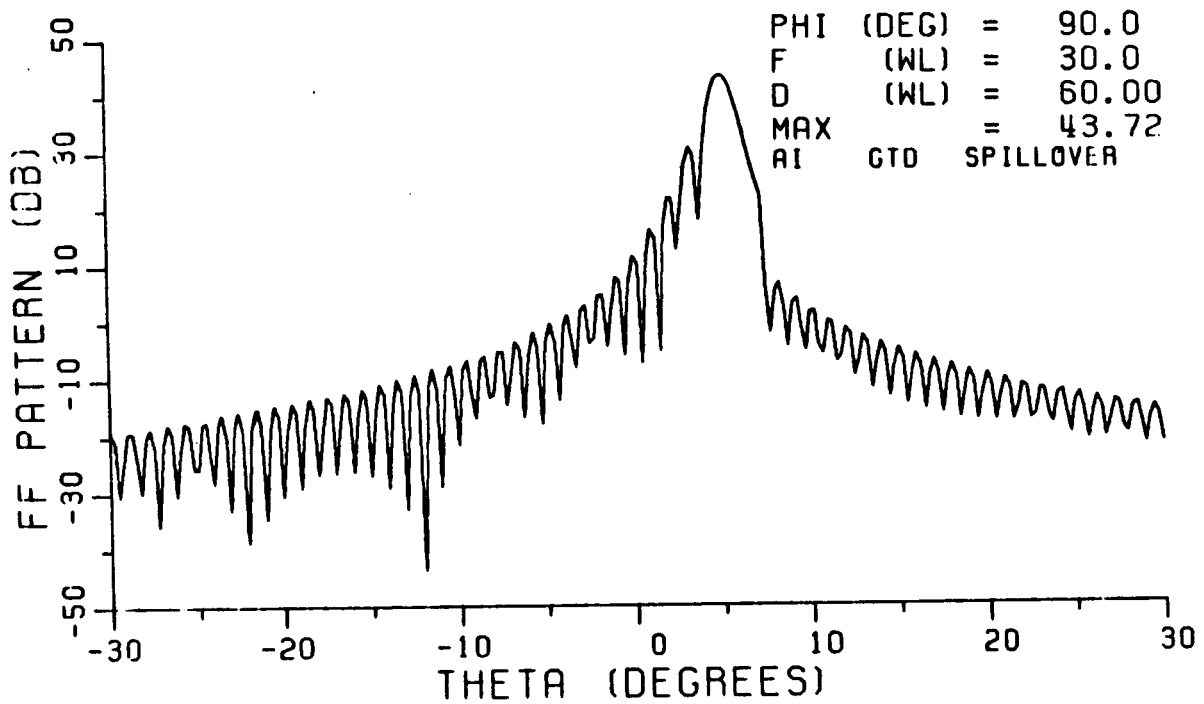
Figure 15. Radiation pattern of the antenna in y-z plane when the feed is (0., -3λ, 0.) away from the focus.
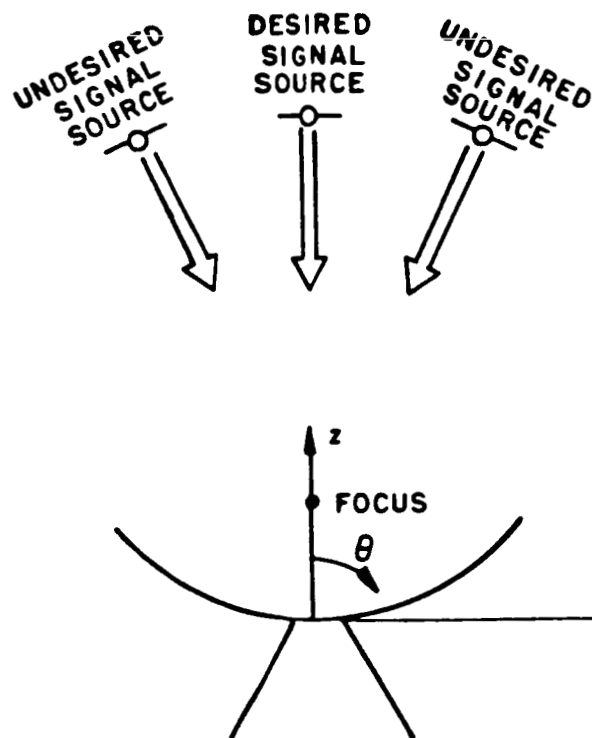
Figure 16. Source distribution in a satellite communication system.
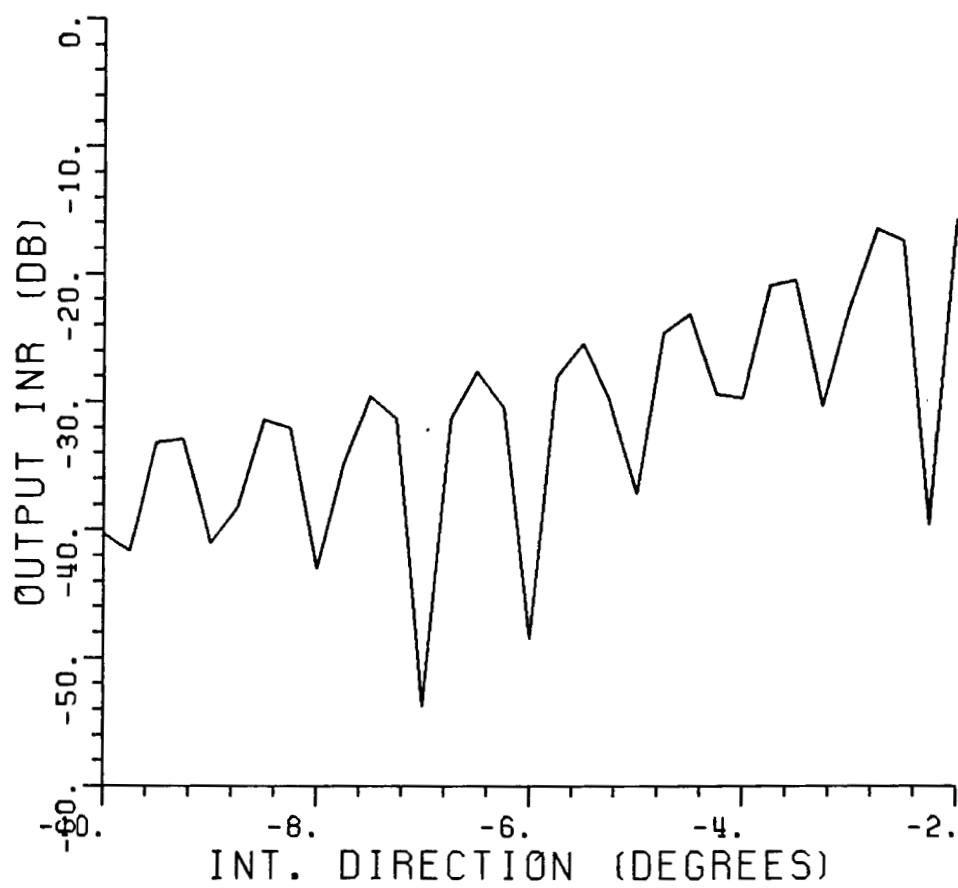
Figure 17. INR at the output of the feed at the focus vs. interfering signal direction. INR (isotropic) = -30 dB.
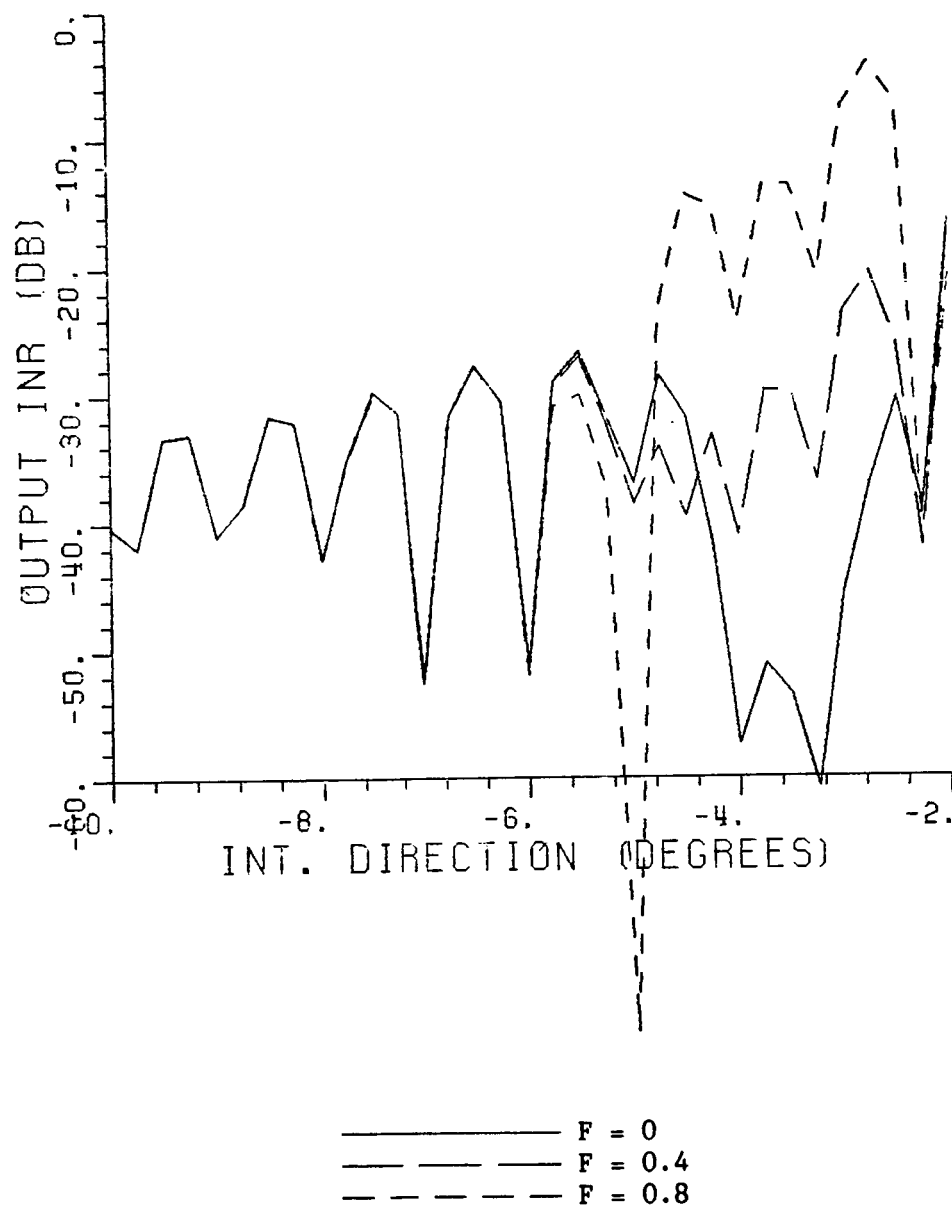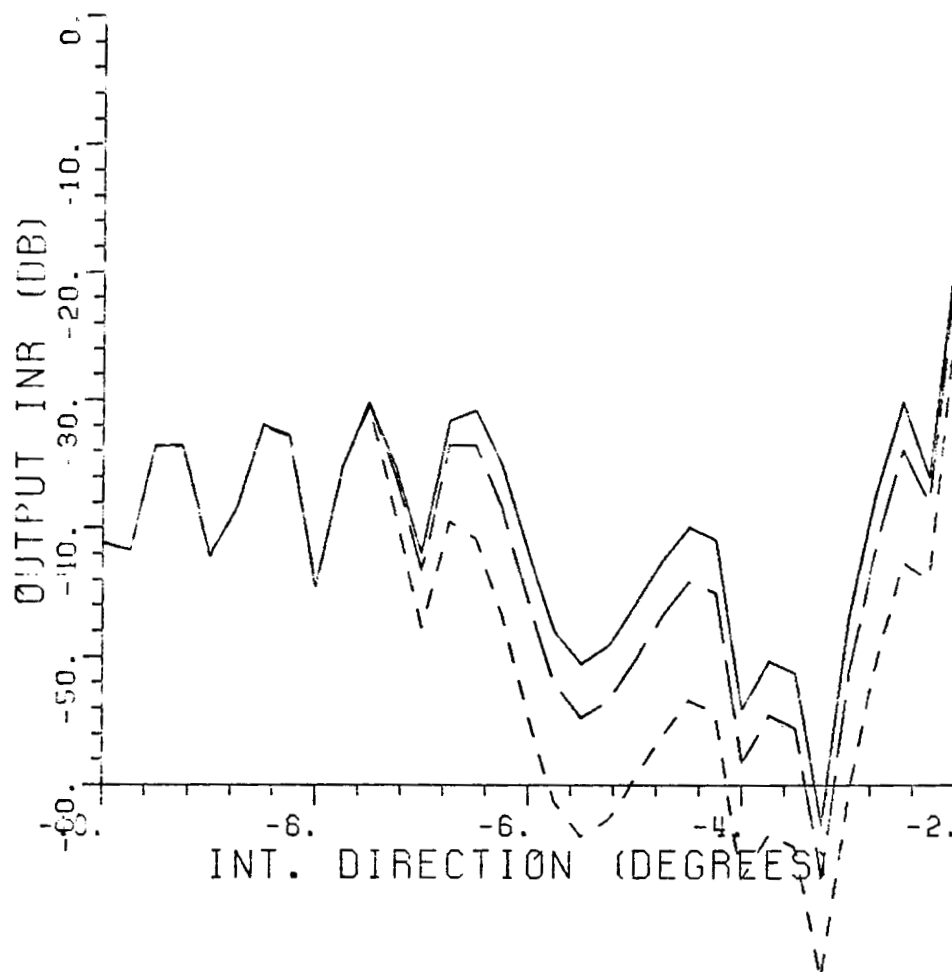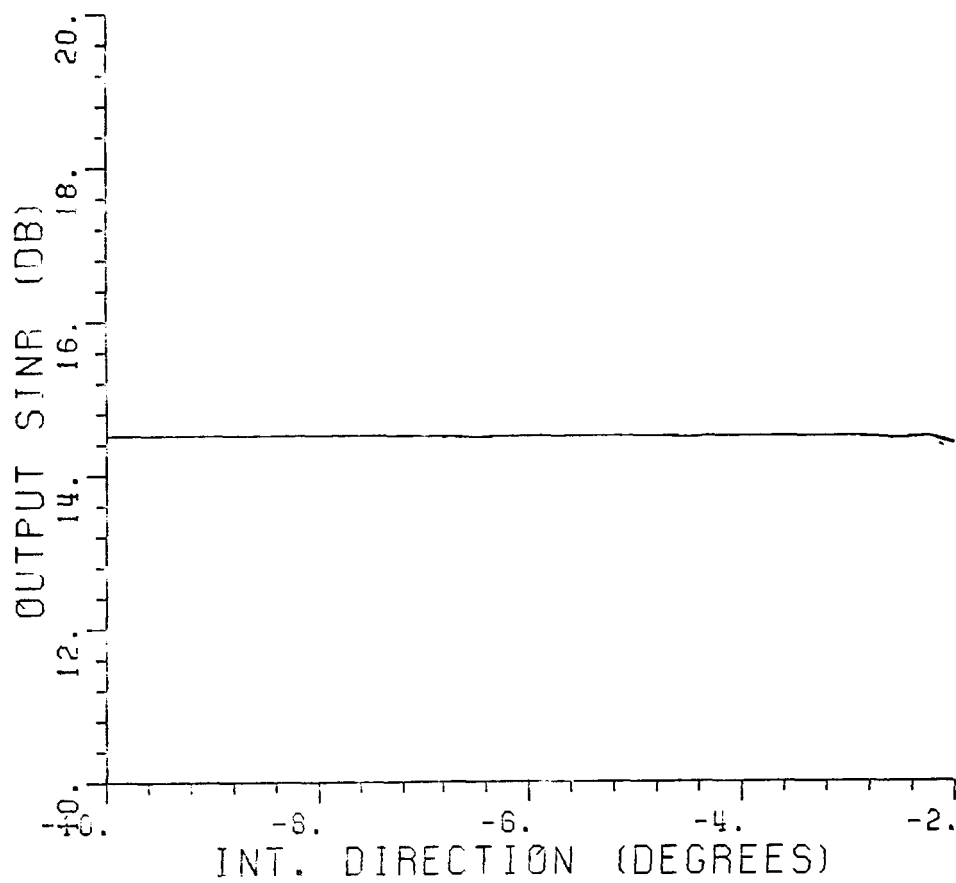
Figure 18. Output INR of a two-element adaptive array vs. interfering signal direction. One defocused feed at (0., 2λ, 0.), INR (isotropic) = -30 dB.

43

Figure 19. Output INR of a three-element adaptive array vs. interfering signal direction. Two defocused feeds at (0., 2λ, 0.) and (0., 3λ, 0.), respectively and INR (isotropic) = -30 dB.

44

Figure 20. Output SINR of a three-element adaptive array vs. interfering signal direction. Two defocused feeds at (0., 2λ, 0.) and (0., 3λ, 0.), respectively and INR (isotropic) = -30 dB.
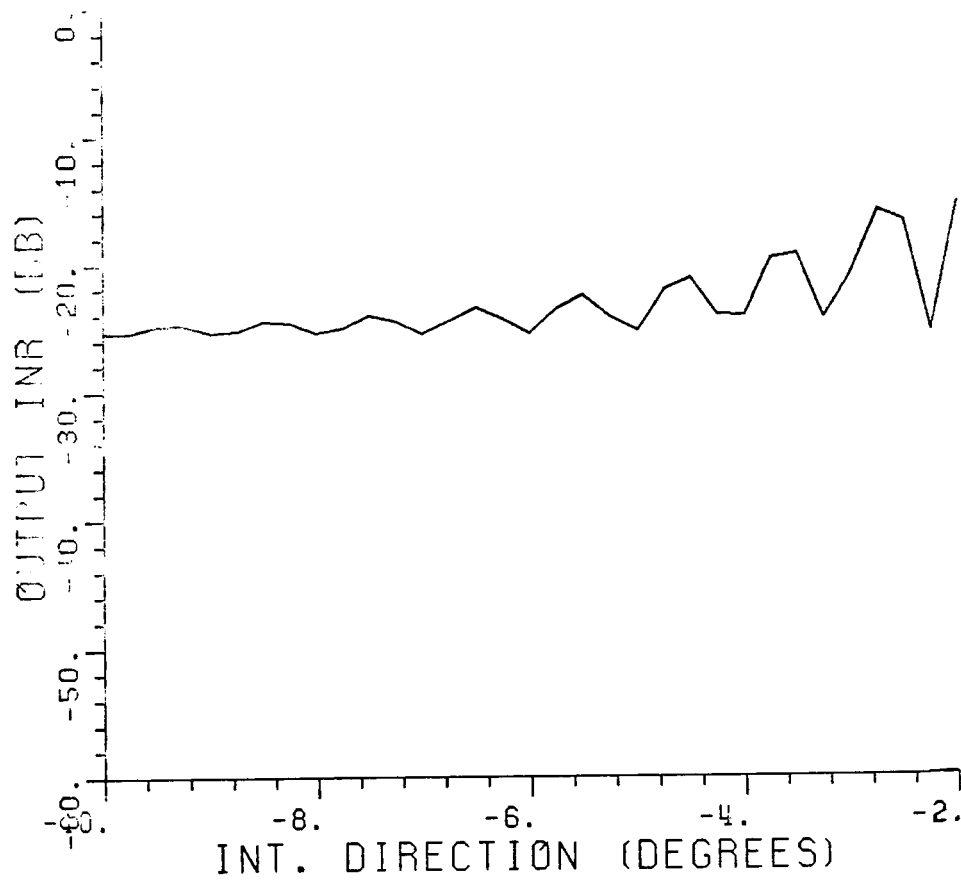
45

Figure 21. INR at the output of the feed at the focus vs. swept
interference signal direction. Two interference signals.
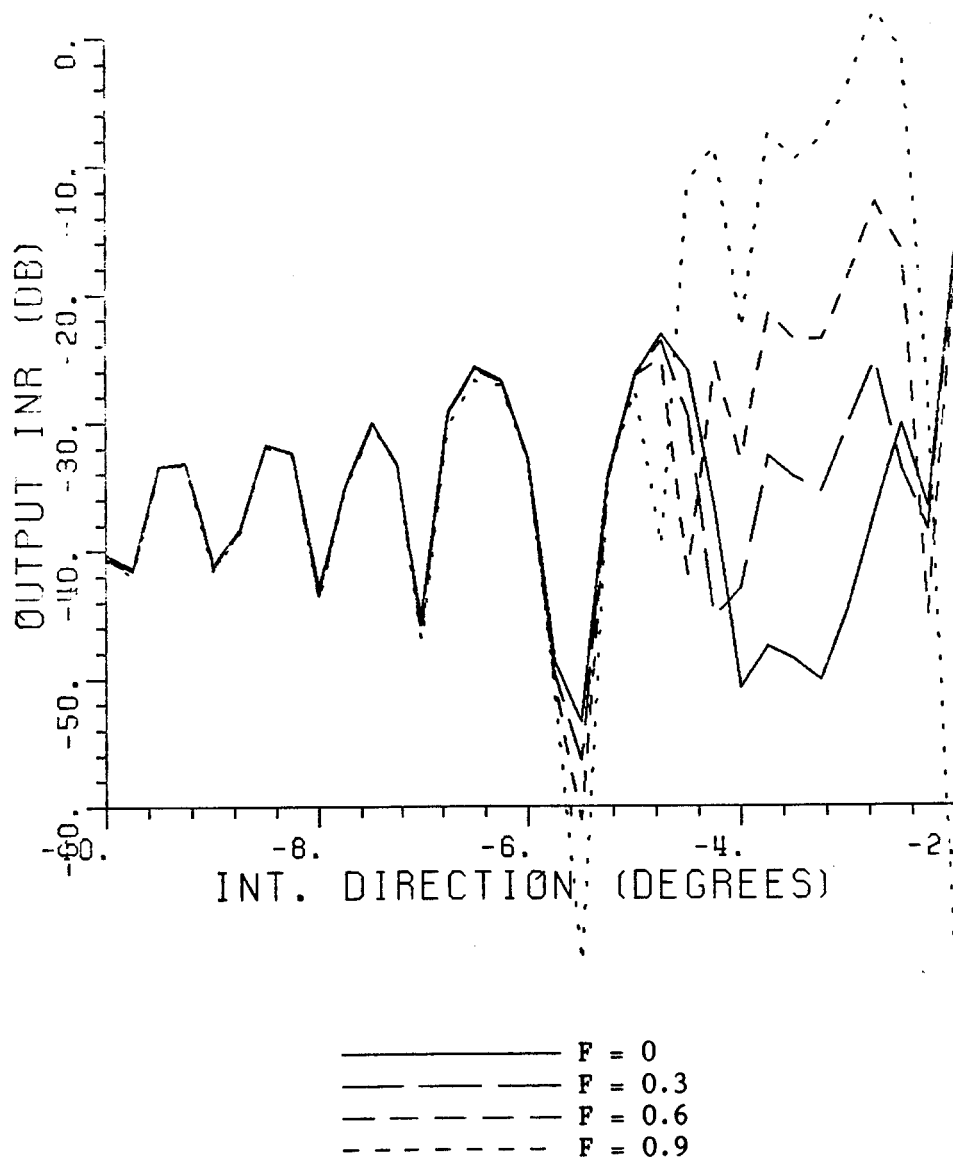θ_{i1}=-5.5°, INR (isotropic) for each interfering signal
= -30 dB.

46

Figure 22. Output INR of a three element adaptive array vs. swept interference signal direction. Two defocused feeds at (0., 2λ, 0.) and (0., 3λ, 0.), respectively. Other parameters are the same as in Figure 21.

47

Figure 23. Output INR of a four-element adaptive array vs. swept
interference signal direction. Three defocused feeds at
(0., 2λ, 0.), (0., 3λ, 0.), and (0., -3λ, 0.), respectively.
Other parameters are the same as in Figure 21.

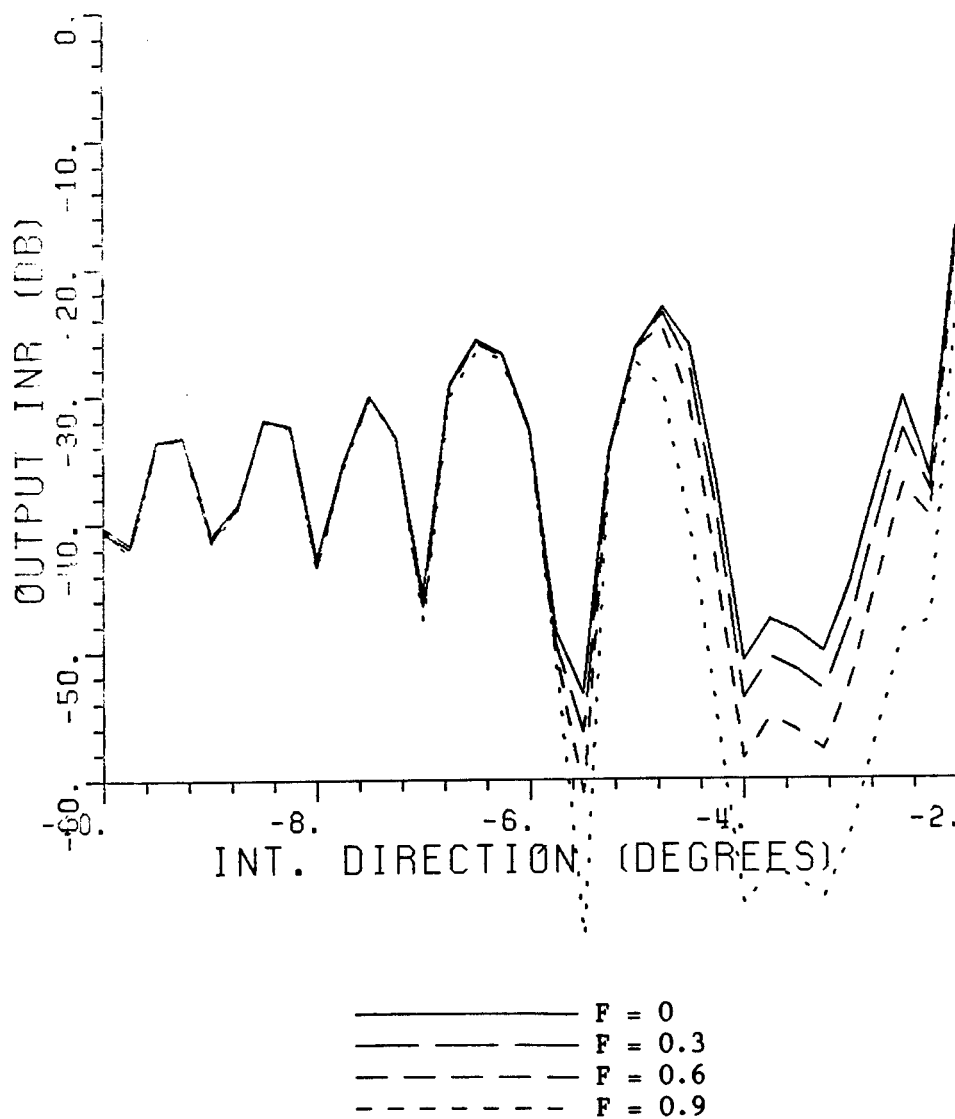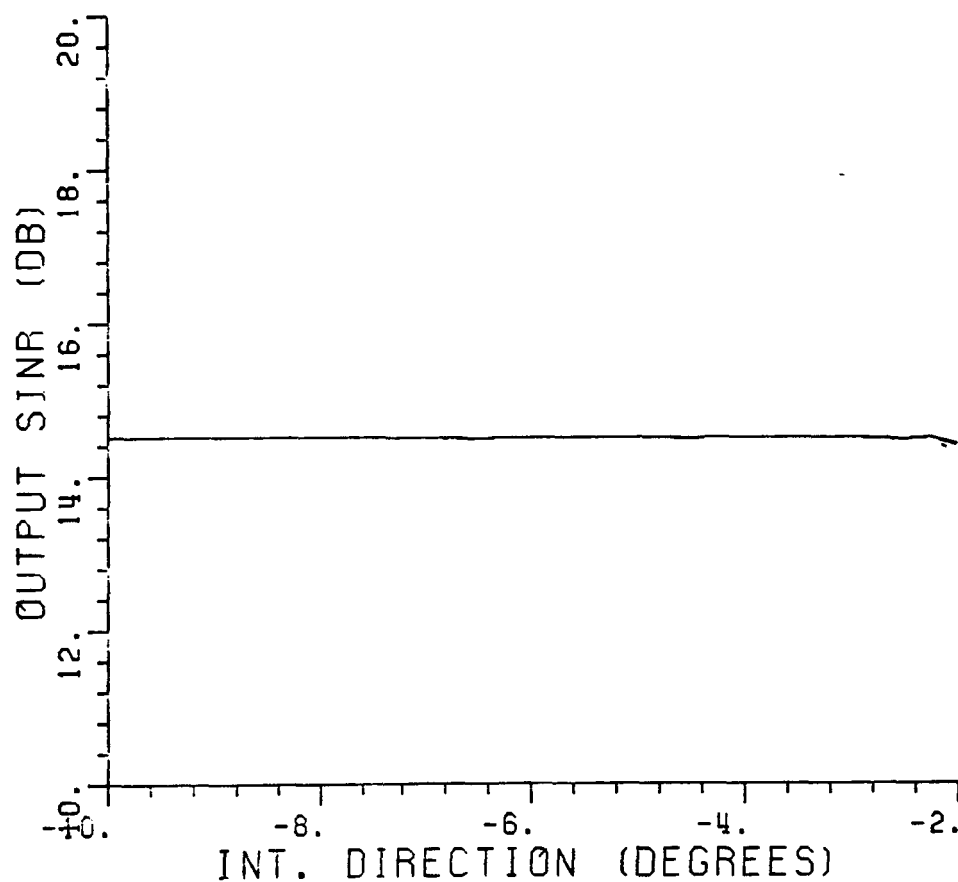Figure 24. Output SINR of a four-element adaptive array vs. swept
interference signal direction. Three defocused feeds at
(0., 2λ, 0.), (0., 3λ, 0.), and (0., -3λ, 0.), respectively.
Other parameters are the same as in Figure 21.

49

REFERENCES

[1] B. Widrow, P.E. Mantey, L.J. Griffiths and B.B. Goode, "Adaptive Antenna Systems," Proceedings of the IEEE, Vol. 55, No. 12, pp. 2143-2159, December 1967.

[2] S.P. Applebaum, "Adaptive Arrays," IEEE Trans. on Antennas and Propagation, Vol. AP-24, No. 5, pp. 585-598, September 1976.

[3] C.L. Zahm, "Application of Adaptive Arrays to Suppress Strong Jammers in the Presence of Weak Signals," IEEE Trans. on Aerospace and Electronic Systems, Vol. AES-9, No. 2, pp. 260-271, March 1973.

[4] R.L. Riegler and R.T. Compton, Jr., "An Adaptive Array for Interference Rejection," Proceedings of the IEEE, Vol. 61, No. 6, pp. 748-758, June 1973.

[5] R.T. Compton, Jr., R.J. Huff, W.G. Swarner and A.A. Ksienski, "Adaptive Arrays for Communication Systems: An Overview of Research at the Ohio State University," IEEE Trans. on Antennas and Propagation, Vol. AP-24, No. 5, pp. 599-607, September 1976.

[6] I.J. Gupta and A.A. Ksienski, "Adaptive Arrays for Satellite Communications," Technical Report 716111-1, June 1984, The Ohio State University ElectroScience Laboratory, Department of Electrical Engineering, prepared under Grant NAG3-536 for NASA/ Lewis Research Center, Cleveland, Ohio.

[7] I.J. Gupta, "Adaptive Antenna Arrays for Weak Interfering Signals," Technical Report 716111-2, January 1985, The Ohio State University ElectroScience Laboratory, Department of Electrical Engineering, prepared under Grant NAG3-536 for NASA/Lewis Research Center, Cleveland, Ohio.

[8] R.A. Mozingo and T.W. Miller, Introduction to Adaptive Arrays, John Wiley and Sons, New York, 1980.

[9] I.S. Reed, J.D. Mallett and L.E. Brennan, "Rapid Convergence Rate in Adaptive Arrays," IEEE Trans. on Aerospace and Electronic Systems, Vol. AES-10, No. 6, pp. 853-863, November 1974.

[10] R.T. Compton, Jr., "On Eigenvalues, SINR, and Element Patterns in Adaptive Arrays," IEEE Trans. on Antennas and Propagation, Vol. AP-32, No. 6, pp. 643-647, June 1984.

[11] R.C. Rudduck and Y.C. Chang, "Numerical Electromagnetic Code-Reflector Antenna Code, Part I: User's Manual (Version 2)," Technical Report 712242-16 (713742), December 1982, The Ohio State University ElectroScience Laboratory, Department of Electrical Engineering, prepared under Contract N00123-79-C-1469 for Naval Regional Procurement Office.

[12] Y.C. Chang and R.C. Rudduck, "Numerical Electromagnetic Code –
Reflector Antenna Code, Part II: Code Manual (Version 2),"
Technical Report 712242-17 (713742), December 1982, The Ohio State
University ElectroScience Laboratory, Department of Electrical
Engineering, prepared under Contract N00123-79-C-1469 for Naval
Regional Procurement Office.